Generation and Detection of a Sub-Poissonian Atom Number Distribution in a One-Dimensional Optical Lattice

J.-B. Béguin, E. M. Bookjans, S. L. Christensen, H. L. Sørensen, J. H. Müller, E. S. Polzik,* and J. Appel†
QUANTOP, Niels Bohr Institute, University of Copenhagen, Blegdamsvej 17, 2100 Copenhagen, Denmark
(Received 8 August 2014; published 30 December 2014)

We demonstrate preparation and detection of an atom number distribution in a one-dimensional atomic lattice with the variance −14 dB below the Poissonian noise level. A mesoscopic ensemble containing a few thousand atoms is trapped in the evanescent field of a nanofiber. The atom number is measured through dual-color homodyne interferometry with a pW-power shot noise limited probe. Strong coupling of the evanescent probe guided by the nanofiber allows for a real-time measurement with a precision of ±8 atoms on an ensemble of some 10^3 atoms in a one-dimensional trap. The method is very well suited for generating collective atomic entangled or spin-squeezed states via a quantum nondemolition measurement as well as for tomography of exotic atomic states in a one-dimensional lattice.

DOI: 10.1103/PhysRevLett.113.263603 PACS numbers: 42.50.Ct, 37.10.Jk, 42.50.Ex

Atoms trapped in an optical lattice are a well-pursued platform for the realization of a quantum simulator and quantum information processing devices [1]. In addition, mesoscopic ensembles of periodically well-separated atoms strongly coupled to light are an excellent arrangement for quantum metrology and sensing applications using collective atomic state entanglement [2].

The recent spectacular progress with cold atoms trapped in the evanescent field emanating from a tapered optical nanofiber with a subwavelength diameter [3–6] offers a realistic and promising implementation of a one-dimensional (1D) optical lattice efficiently coupled to a single well-defined light mode. Together with the mature technology of interconnecting optical fibers, atomic ensembles trapped around nanofibers have the potential to play an integral part in the construction of complex quantum networks. Photons propagating in a fiber connect hybrid quantum systems by interacting with various realizations of quantum systems, such as solid state systems and atoms, through strong light-matter coupling at nanotapered fiber nodes [7,8].

An efficient quantum interface between light and collective degrees of freedom of an atomic ensemble requires a high optical depth and a measurement sensitivity limited by the shot noise of light and the projection noise of atoms [9]. Under these conditions, a quantum nondemolition (QND) measurement of atomic population differences has been used for the generation of spin squeezed [10], entangled states to improve atomic clocks [11,12] and magnetometers [13,14]. In addition, optical probing of atoms in one-dimensional lattices with sub-Poissonan precision has been proposed as a valuable measurement tool for strongly correlated systems [15]. The preparation of ensembles with narrow atom number distribution in atom traps and the knowledge of its statistics in real time is also a well-recognized goal for quantum gate implementations based on collective Rydberg excitations [16,17] or atomic Bragg mirrors [18]. For these and other applications, it is desirable to have a probing and preparation method at hand which not only is minimally destructive but also widely tunable in bandwidth. Ideally, it should enable monitoring dynamics on different time scales and to outrun the influence of any decoherence not caused by the measurement itself. While impressive atom number resolution has been reported for atomic ensembles inhomogeneously coupled to an optical cavity mode [19] and for ensembles trapped inside a low-noise magneto-optical trap [20], we demonstrate a fast single-pass atom number measurement method that is readily adapted to different measurement and preparation tasks in 1D ensembles.

In this Letter, we realize the first real-time, minimally destructive detection of atoms with sub-Poissonian sensitivity in a 1D nanofiber lattice trap. Due to the guiding of the probe light by the nanofiber, the optical depth $N_{\mathrm{at}}\sigma/A$ achieves maximal values for a given atom number N_{at} as the light beam cross section A becomes comparable to the atomic cross section. The minimally destructive measurement is achieved by balancing the phase information obtained from atoms against the measurement backaction, combined with quantum noise limited sensitivity for both probe photons and atoms. Through a continuous shot noise limited measurement of the atom induced phase shift of light, we resolve and prepare an atom number distribution of the ensemble with a minimum Fano factor $(\Delta N_{\mathrm{at}})^2/N_{\mathrm{at}}$ of −14 dB. The reduction of the atom number noise compared to the Poisson distribution is ultimately limited only by probe induced stochastic loss of atoms [21–23]. The absolute number of atoms in the lattice trap is calibrated accurately via a robust experimental method based on optical pumping [24]. Finally, we show that the achieved light-atom coupling strength and quantum noise limited sensitivity is suitable for quantum state tomography

and will allow for the generation of many-body entangled states by QND measurements in our system.

In the experiment, Cesium atoms are prepared in a nanofiber trap. Two counter-propagating red-detuned fields with a wavelength of $\lambda_{\mathrm{red}} = 1057$ nm and a total power of $P_{\mathrm{red}} = 2 \times 1$ mW together with an orthogonally linearly polarized blue-detuned running-wave field (with $\lambda_{\mathrm{blue}} = 780$ nm, $P_{\mathrm{blue}} = 10$ mW) are sent through an optical nanofiber and form two one-dimensional optical lattices [4]. With a nominal nanofiber diameter of $d = 500$ nm, the trapping sites are located 200 nm above the surface of the fiber. A magneto-optical trap (MOT) is superimposed on the fiber; atoms are loaded into the lattice trap after a sub-Doppler cooling phase, during which they are pumped into the hyperfine ground state $|3\rangle \equiv (6^2S_{1/2}, F = 3)$. Immediately before probing, the atoms are pumped back to the $|4\rangle \equiv (6^2S_{1/2}, F = 4)$ state with external repuming light tuned to the $|3\rangle \rightarrow |4'\rangle \equiv (6^2P_{3/2}, F = 4)$ transition.

Our atom number preparation and real-time measurement procedure relies on the detection of a differential phase shift imprinted by the atoms on two probe light fields propagating in the fundamental mode of the fiber. The two probes are detuned symmetrically around the atomic resonance by $\pm\Omega$, balanced in power, and linearly polarized as the 1057 nm trap field. They are generated from an acousto-optic modulator (AOM) in the Raman-Nath regime before they are recombined in a common spatial mode, see Fig. 1(a). Due to the antisymmetric nature of the atomic dispersion [Fig. 1(b)], the probes have acquired phase shifts of opposite sign after interacting with the atoms at the fiber nanotaper. Measuring the differential phase shift between the two probes yields a signal proportional to the number of interacting atoms. At the same time, any common-mode optical path length and polarization fluctuation noise is canceled. Furthermore, inhomogeneous differential Stark shifts imprinted on the atoms by off resonant probing are suppressed [25].

After passage through the atomic ensemble, the differential phase shift between the two probes is measured using optical homodyne interferometry, see Fig. 1(a); the two probes are overlapped with a strong optical local oscillator (LO) on a 90:10 beam splitter, and the signal is detected with a photodetector peaked around the beat-note frequency Ω. Because of the symmetrical placement of the probe sidebands with respect to the LO, the usual 3 dB noise penalty for heterodyne detection is avoided [26]. The detected beat note in the photocurrent is mixed down to baseband electronically and both differential phase shift and common-mode attenuation of the probe light are extracted from the signal. All optical fields used for probing are derived from the same laser source and the optical phase of the LO is stabilized to the point of highest differential phase sensitivity by a slow servo loop.

Since in homodyne detection the signal strength and the photon shot noise contribution from the LO scale

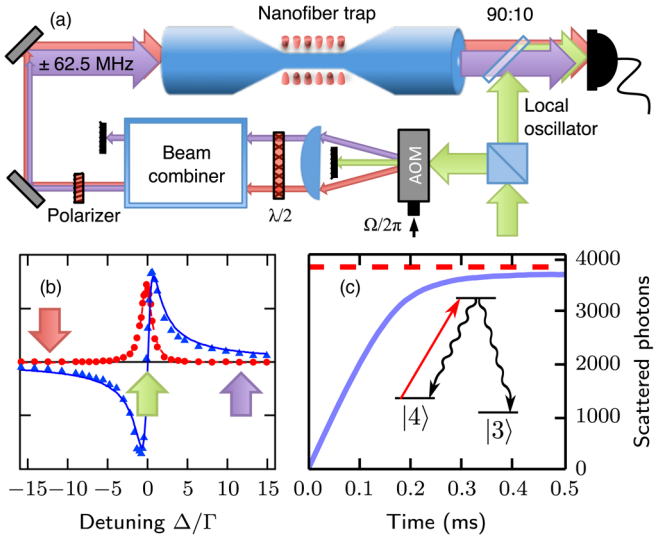

FIG. 1 (color online). (a) Experimental setup. Two 1D optical lattices are formed in the nanofiber trap by two trapping beams (not shown). Two probe beams with fixed frequency difference are generated with an AOM and then coupled into the nanofiber where they interact with the atomic ensemble. They interfere with a strong LO on a 90:10-beam splitter and a homodyne measurement is performed. (b) Absorption (red dots) and dispersion signals (blue triangles) measured with trapped atoms; arrows indicate probe and LO frequencies. (c) Atom number calibration. Resonant light pumps atoms from $|4\rangle$ to $|3\rangle$. The total number of trapped atoms is determined from the decay branching ratio (see inset) and the asymptote (red dashed line) of the cumulative number of scattered photons (solid blue line, average of 200 experiments).

identically, technical noise sources can be overcome in a high detection bandwidth by using a sufficiently high LO power. The ultimate signal-to-noise ratio (SNR) with coherent light states is therefore only limited by the intrinsic quantum noise of the probes. In our experiment, LO photon shot noise dominates residual electronic noise typically by a factor of 3.5. This, together with other imperfections, translates into a minimum phase uncertainty $\delta\varphi$ slightly above the standard quantum limit expressed as

$$\delta\varphi = \frac{1}{2\sqrt{qN_{\mathrm{ph}}}}, \qquad q \equiv \epsilon(1-l)\mathcal{V}\eta. \tag{1}$$

Here, N_{ph} is the total number of probe photons at the atoms during the measurement probe time and q is an overall quantum efficiency, dependent on the quantum efficiency of the detector ϵ, the losses of the probe from the atoms to the detector l, the mode overlap of the probes and LO at the detector $\mathcal{V}$, and the ratio η of the LO shot noise to total detection noise [27]. A value of $q = 0.40 \pm 0.04$ is achieved in the experimental setup. We have verified the modeled performance of the detection scheme by a measurement of the Allan deviation of interferometer phase

in the absence of fiber-trapped atoms (for details, see [28]: dual-color homodyne detection).

By simply blocking one of the probe sidebands, the measurement scheme turns into standard heterodyne detection, which is used for initial calibration purposes [30]. With the remaining sideband tuned around the $|4\rangle \rightarrow |5'\rangle \equiv (6^2P_{3/2}, F' = 5)$ transition, the line shape and position of the optical resonance for trapped atoms is observed [see Fig. 1(b)]. An energy absorption measurement with a single probe tuned to the $|4\rangle \rightarrow |4'\rangle$ transition is used to calibrate the number of trapped atoms. In other nanofiber trap experiments, the number of atoms has been estimated from the absorbed power of a probe beam fully saturating the trapped atoms [4,5]. We apply a similarly robust but faster method, which allows us to measure the atom number in a single run with adequate resolution and good accuracy, by recording optical pumping transients [31], (see also [28]: atom number calibration method). Atoms excited to the $|4'\rangle$ level decay with a fixed branching ratio into the $|4\rangle$ and $|3\rangle$ ground levels which allows us to determine the number of atoms from the number of absorbed probe photons. From an average over 178 consecutive experimental runs, as shown in Fig. 1(c), we find for the average number of trapped atoms $N_{\mathrm{at}} = 1606 \pm 4^{\mathrm{stat}} \pm 160^{\mathrm{sys}}$. The systematic error for this measurement is dominated by the fractional uncertainty of the overall quantum efficiency q.

To achieve the highest atomic response for the dual-color dispersive measurement, the probes address the atoms in the $|4\rangle$ state through the excited $|5'\rangle$ state. We detune the probes by $\Omega = \pm 2\pi \times 62.5$ MHz $\approx \pm 12\Gamma$ from the atomic transition, where $\Gamma = 2\pi \times 5.23$ MHz is the natural linewidth. This choice renders the atomic sample sufficiently transparent to couple all atoms equally while keeping the influence of neighboring hyperfine levels small. From the measured phase shift for ensembles with calibrated atom number, we infer an on resonant optical depth of $\alpha_{\mathrm{at}} = 0.024$ for a single maximally polarized atom on the $|4\rangle \rightarrow |5'\rangle$ transition [32]. Comparing to earlier results obtained in a free space optical dipole trap with a related probing method [33], this represents an improvement of more than 2 orders of magnitude in the signal from a single atom.

To illustrate the wide tunability of strength and bandwidth of the measurement, we show real-time measurements of the atomic phase shift probing on the $|4\rangle \rightarrow |5'\rangle$ transition with and without external repumping light for varying probe powers in Fig. 2. In the shown range, the maximum observed atomic phase shift is independent of the probe power as expected from the calculated saturation power of 224 nW at the used probe detuning. The probe-induced signal decay can be made much faster than the unperturbed trap lifetime without compromising signal strength by saturating the atoms. The data presented in Fig. 2 are taken on a trap with $1/e$ lifetime in the absence of probing of $\tau_{\mathrm{bg}} = 6.8$ ms [34]. Curiously, we observe that the probe induced loss rate grows slower than linear

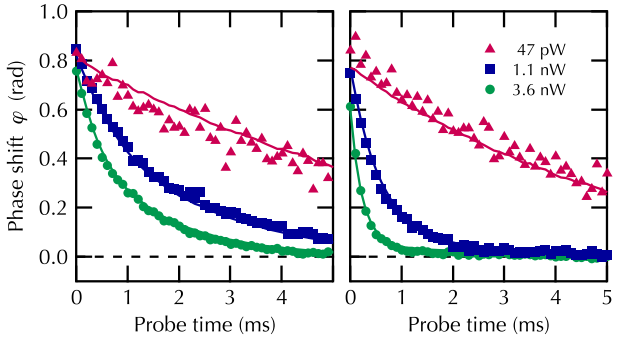

FIG. 2 (color online). Atom induced phase shift measured with weak coherent probe light of different powers. Symbols: each trace depicts real-time phase shift data, acquired with a 100 kHz detection bandwidth in a single lattice trap realization; Solid lines: average over 200 realizations. Using the same set of probe powers (see legend), data in the left (right) panel were recorded with (without) external repumping light present. Probing starts 1 ms after trap loading.

with the photon flux. The average numbers of scattering events n_{heat} to remove an atom from the trap are found to be $n_{\mathrm{heat}} \simeq 380$ for $P = 3.6$ nW, while $n_{\mathrm{heat}} \simeq 190$ for $P = 1.1$ nW, and $n_{\mathrm{heat}} \simeq 56$ only for $P = 0.15$ nW. Plain recoil heating in individual trap sites of calculated depth $10^3\ E_{\mathrm{recoil}}$ predicts constant $n_{\mathrm{heat}} \simeq 500$ [35] and clearly cannot explain the data. This peculiar behavior is not understood at present and is subject to further studies. In the absence of repumping light, probe-induced hyperfine pumping into the atomic state $|3\rangle$ is observed on average after $n_{\mathrm{hf}} = 67$ spontaneous emission events, in good agreement with the calculated value at the used probe detuning.

We now apply the calibrated dispersive minimally destructive probing method to prepare atom number distributions in the optical lattice with sub-Poissonian fluctuations. The Fano factor quantifies the reduction in the atom number fluctuations as compared to a Poisson distribution as $F = (\Delta N_{\mathrm{at}})^2/\langle N_{\mathrm{at}}\rangle$. A Fano factor below unity is sometimes referred to as number squeezing. In the experiment, atoms are probed 10 ms after the sub-Doppler cooling to avoid transit signals from untrapped atoms from the initial MOT reservoir. Atoms are probed on the $|4\rangle \rightarrow |5'\rangle$ transition and external repumping light on the $|3\rangle \rightarrow |4'\rangle$ transition is used to counteract hyperfine pumping. In Fig. 3, we show a typical record of the measured real-time phase shift from a single realization where data points are averaged over 5 μs. The noisy data are seen to follow a smoothly decaying curve with time or equivalently, the probe photon number. We apply a recursive Bayesian estimation procedure to track the atom number distribution at a given invested probe photon number N_{ph} from all phase measurement data up to that time (see [28]: recursive Bayesian estimation of the atom number): we describe our knowledge of the atom number by an initially uniform

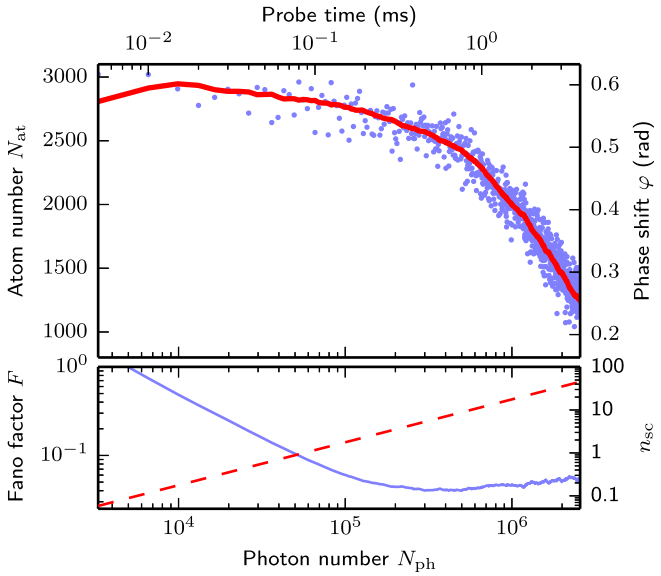

FIG. 3 (color online). Top: recursive Bayesian estimation of the atom number distribution. Blue dots: atom induced optical phase shift φ, as measured in a single experiment with the dual-color homodyne technique. Red line: mean of the estimated probability distribution for N_{at} at every time. Bottom: solid blue line: Fano factor $F = \mathrm{var}(N_{at})/\langle N_{at}\rangle$ from the same probability distribution. Dashed red line: number of scattered photons n_{sc} per atom (see main text). All data were recorded with a probe power of 154 pW, 10 ms after the MOT cooling phase.

probability distribution. With every sample of acquired, shot noise-contaminated data, we update this distribution using Bayes rule of inference. In every step, we evolve our estimator distribution to account for stochastic loss of atoms due to background gas collisions and due to heating by the probe light. The lower panel in Fig. 3 displays the Fano factor for the atom number estimator. We find a minimum Fano factor of -14 dB from the knowledge acquired by 5×10^5 probe photons which led to a loss of only 14% of the initial atoms. This demonstrates that we can prepare ensembles with arbitrary atom numbers between 1000–2500 with Fano factors well below -10 dB.

For the preparation of the total trapped atom number, a strong measurement can be applied, since the only back-action mechanism changing the variable of interest is atom loss due to recoil heating. Tomographic characterization of collective atomic hyperfine coherence by measuring atomic population differences instead does not allow for the use of repump light [36]. Preparation of spin-squeezed ensembles by a QND measurement is even more stringent and limits the number of allowed spontaneous emission events below unity [10,12].

We use a simplified model for the variance of the atom number estimator, inspired by [19], in order to evaluate the potential of the measurement scheme for the different tasks. Assuming that all atom loss is caused by probe light, the variance of the estimator writes as

$$(\Delta N_{at})^2 = \left[\frac{1}{(\Delta N_{at}^{i})^2} + q\alpha_{at} n_{sc}\right]^{-1} + N_{at}\frac{n_{sc}}{n_{loss}}. \quad (2)$$

Here, α_{at} denotes the single-atom optical depth on the probe transition, n_{sc} is the number of probe photons scattered into free space for a single atom, $(\Delta N_{at}^{i})^2$ is the initial variance of the atomic ensemble before probing, and n_{loss} the critical number of scattering events, i.e., $n_{heat} = 56$ for atom number preparation as in Fig. 3, $(n_{hf}^{-1} + n_{heat}^{-1})^{-1}$ for state tomography and $n_{loss} \lesssim 1$ for conditional spin-squeezing. Any initial information about the atom number distribution is encoded in the prior variance $(\Delta N_{at}^{i})^2$. The first term describes the gain of knowledge from the phase shift measurement while the second term reflects the noise from stochastic atom loss.

The measurement strength characterized by n_{sc}, can now be optimized for all three tasks (see [28]: simplified model for atom number estimator variance). For atom number preparation, we find $n_{sc} = 2.4$ leading to a predicted minimum Fano factor of -11 dB for the parameters of Fig. 3. The simple model is somewhat pessimistic but still in reasonable agreement with the observed values.

In quantum state tomography where reduction of the variance has to be balanced with the noise introduced by heating and hyperfine pumping, the minimum predicted Fano factor is -8 dB. This should be compared with -3 dB required to observe negative Wigner function ensemble distributions and hence, allows characterization of non-classical spin states for ensembles containing 2500 atoms. Extrapolating to measurement-based preparation of spin-squeezed collective atomic states, where we need to take the damping of hyperfine coherence due to photon scattering into account, we find that metrologically relevant squeezing up to -4.2 dB in our system is achievable if all other decoherence channels are negligible.

In conclusion, we have demonstrated an efficient interface between fiber-guided light modes and atomic ensembles trapped in a 1D optical lattice. The nanofiber trap geometry offers two obvious routes for future improvements. The single atom coupling strength can be moderately increased by pulling atoms closer to the fiber surface, but also substantially increased by embedding the trap into an optical resonator using integrated fiber Bragg gratings [7,37]. Alternatively, the ensemble size can be increased by simply using longer fiber sections without compromising the single atom coupling. At least one order of magnitude larger ensembles are realistic with current state of the art nanofiber production technology.

We gratefully acknowledge Professor A. Rauschenbeutel and his group for advice and access to their fiber pulling rig and thank Professor M. F. Andersen for fruitful and enlightening discussions. This work has been supported by the ERC Grant INTERFACE, the US ARO Grant No. W911NF-11-0235, the EU Grant SIQS, and MALICIA.

*Corresponding author.
polzik@nbi.dk
†Corresponding author.
jappel@nbi.dk

[1] I. Bloch, J. Dalibard, and S. Nascimbène, Nat. Phys. **8**, 267 (2012).
[2] V. Giovannetti, S. Lloyd, and L. Maccone, Nat. Photonics **5**, 222 (2011).
[3] F. Le Kien, V. I. Balykin, and K. Hakuta, Phys. Rev. A **70**, 063403 (2004).
[4] E. Vetsch, D. Reitz, G. Sagué, R. Schmidt, S. T. Dawkins, and A. Rauschenbeutel, Phys. Rev. Lett. **104**, 203603 (2010).
[5] A. Goban, K. S. Choi, D. J. Alton, D. Ding, C. Lacroûte, M. Pototschnig, T. Thiele, N. P. Stern, and H. J. Kimble, Phys. Rev. Lett. **109**, 033603 (2012).
[6] S. T. Dawkins, R. Mitsch, D. Reitz, E. Vetsch, and A. Rauschenbeutel, Phys. Rev. Lett. **107**, 243601 (2011).
[7] K. P. Nayak, P. Zhang, and K. Hakuta, Opt. Lett. **39**, 232 (2014).
[8] M. Hafezi, Z. Kim, S. L. Rolston, L. A. Orozco, B. L. Lev, and J. M. Taylor, Phys. Rev. A **85**, 020302 (2012).
[9] K. Hammerer, A. S. Sørensen, and E. S. Polzik, Rev. Mod. Phys. **82**, 1041 (2010).
[10] J. Appel, P. J. Windpassinger, D. Oblak, U. Busk Hoff, N. Kjærgaard, and E. S. Polzik, Proc. Natl. Acad. Sci. U.S.A. **106**, 10960 (2009).
[11] A. Louchet-Chauvet, J. Appel, J. J. Renema, D. Oblak, N. Kjaergaard, and E. S. Polzik, New J. Phys. **12**, 065032 (2010).
[12] M. H. Schleier-Smith, I. D. Leroux, and V. Vuletić, Phys. Rev. Lett. **104**, 073604 (2010).
[13] W. Wasilewski, K. Jensen, H. Krauter, J. J. Renema, M. V. Balabas, and E. S. Polzik, Phys. Rev. Lett. **104**, 133601 (2010).
[14] M. Koschorreck, M. Napolitano, B. Dubost, and M. W. Mitchell, Phys. Rev. Lett. **104**, 093602 (2010).
[15] K. Eckert, O. Romero-Isart, M. Rodriguez, M. Lewenstein, E. S. Polzik, and A. Sanpera, Nat. Phys. **4**, 50 (2008).
[16] M. Saffman, T. G. Walker, and K. Mølmer, Rev. Mod. Phys. **82**, 2313 (2010).
[17] D. Petrosyan and G. M. Nikolopoulos, Phys. Rev. A **89**, 013419 (2014).
[18] D. E. Chang, L. Jiang, A. V. Gorshkov, and H. J. Kimble, New J. Phys. **14**, 063003 (2012).
[19] H. Zhang, R. McConnell, S. Ćuk, Q. Lin, M. H. Schleier-Smith, I. D. Leroux, and V. Vuletić, Phys. Rev. Lett. **109**, 133603 (2012).
[20] D. B. Hume, I. Stroescu, M. Joos, W. Muessel, H. Strobel, and M. K. Oberthaler, Phys. Rev. Lett. **111**, 253001 (2013).
[21] A. Itah, H. Veksler, O. Lahav, A. Blumkin, C. Moreno, C. Gordon, and J. Steinhauer, Phys. Rev. Lett. **104**, 113001 (2010).
[22] Y. R. P. Sortais, A. Fuhrmanek, R. Bourgain, and A. Browaeys, Phys. Rev. A **85**, 035403 (2012).
[23] S. Whitlock, C. F. Ockeloen, and R. J. C. Spreeuw, Phys. Rev. Lett. **104**, 120402 (2010).
[24] W. Ketterle, K. B. Davis, M. A. Joffe, A. Martin, and D. E. Pritchard, Phys. Rev. Lett. **70**, 2253 (1993).
[25] M. Saffman, D. Oblak, J. Appel, and E. S. Polzik, Phys. Rev. A **79**, 023831 (2009).
[26] M. Locke and C. Fertig, J. Opt. Soc. Am. B **30**, 2409 (2013).
[27] J. Appel, D. Hoffman, E. Figueroa, and A. I. Lvovsky, Phys. Rev. A **75**, 035802 (2007).
[28] See Supplemental Material at http://link.aps.org/supplemental/10.1103/PhysRevLett.113.263603, which includes Ref. [29], for a detailed discussion of the measurement methods and the Bayesian estimation model.
[29] S. Särkkä, *Bayesian Filtering and Smoothing* (Cambridge University Press, Cambridge, England, 2013).
[30] J. M. Pino, R. J. Wild, P. Makotyn, D. S. Jin, and E. A. Cornell, Phys. Rev. A **83**, 033615 (2011).
[31] Y.-C. Chen, Y.-A. Liao, L. Hsu, and I. A. Yu, Phys. Rev. A **64**, 031401 (2001).
[32] We assume here that the dispersively probed ensemble is unpolarized.
[33] S. L. Christensen, J.-B. Béguin, E. Bookjans, H. L. Sørensen, J. H. Müller, J. Appel, and E. S. Polzik, Phys. Rev. A **89**, 033801 (2014).
[34] For the data presented in Fig. 3, intensity noise of the trap lasers has been reduced significantly which led to a longer trap lifetime of 20 ms.
[35] S. Wolf, S. J. Oliver, and D. S. Weiss, Phys. Rev. Lett. **85**, 4249 (2000).
[36] S. L. Christensen, J. B. Béguin, H. L. Sørensen, E. Bookjans, D. Oblak, J. H. Müller, J. Appel, and E. S. Polzik, New J. Phys. **15**, 015002 (2013).
[37] C. Wuttke, M. Becker, S. Brückner, M. Rothhardt, and A. Rauschenbeutel, Opt. Lett. **37**, 1949 (2012).